ESTIMATING THE APPROXIMATION UNCERTAINTY FOR DIGITAL MATERIALS SUBJECTED TO STRESS RELAXATION TESTS

Stanisław Adamczak[1]), Jerzy Bochnia[2])

Kielce University of Technology, Faculty of Mechatronics and Mechanical Engineering, Al. 1000-lecia P. P. 7, 25-314 Kielce, Poland
(✉ adamj@tu.kielce.pl, +48 22 432 7721, jbochnia@tu.kielce.pl)

Abstract

The main aim of the study was to determine the goodness of fit between the relaxation function described with a rheological model and the real (experimental) relaxation curves obtained for digital materials fabricated with a Connex 350 printer using the PolyJet additive manufacturing technology. The study involved estimating the uncertainty of approximation of the parameters of the theoretical relaxation curve. The knowledge of digital materials is not yet sufficient; their properties are not so well-known as those of metallic alloys or plastics used as structural materials. Intensive research is thus required to find out more about their behavior in various conditions. From the calculation results, i.e. the uncertainty of approximation of the relaxation function parameters, it is evident that the experimental curves coincide with the curves obtained by means of the solid model when the approximation uncertainty is taken into account. This suggests that the assumed solid model is well-suited to describe a real material.

Keywords: digital materials, stress relaxation, approximation uncertainty.

1. Introduction

Rapid development of additive manufacturing technologies in recent years is accompanied with improvement of the materials used for this purpose. The new materials being launched in the market differ in physical and mechanical characteristics; it is thus vital to study their behavior in detail. The high-tech materials include digital materials used in the Poly Jet additive manufacturing technology.

Digital materials are fabricated by combining two base resins on the build tray of a 3D printer. Resin drops are placed at precise locations using digital control heads; hence the origin of the materials' name. The most common are base resins commercially known as TangoBlackPlus and VeroWhitePlus. They can be combined in different proportions in order to obtain new materials with different Shore hardness. The TangoBlack materials are rubber-like materials with a high tensile strength. For example, according to their producer (*http://www.stratasys.com/materials/polyjet/digital-materials*), TangoBlackPlus FLX980 has a tensile strength of 0.8–1.5 MPa. The VeroWhite materials, on the other hand, are rigid materials. For instance, Durus White RGD430 is characterized by a tensile strength of 20–30 MPa. It should be mentioned that the values provided in the catalogues are approximate in nature. Materials produced by additive manufacturing exhibit anisotropy depending on the arrangement on the build tray, *i.e.* the printing direction. The details on the subject can be found, for example, in [1−6].

In [1], the uncertainty of tensile strength measurements was calculated taking into account three directions of printing of test pieces made of photo-cured resin (Vero White). The test results were used to assess the innovation risks for additive manufacturing. In [2], the uncertainty of tensile strength measurements was calculated for specimens produced

by additive manufacturing using Full Cure 720. The tests were carried out for a large number of specimens and the results were shown in the form of normal distribution of probability density as a function of tensile strength. The studies were essential to determine the properties of new model materials used in additive manufacturing.

Digital materials are suitable for modelling various elements, e.g. sealing rings, membranes, viscoelastic elements, cable guides, muscle models and other structural components made of polymer-based plastics. Digital materials are well-suited to simulate the most popular plastics, for example, acrylic, PTFE, AS, PA, rubbers, and polyurethanes.

As digital materials exhibit stress relaxation, it is necessary to continue research in this area. Stress relaxation in polymers has been described by many researchers, *e.g.* [7−10]. However, there are no research reports on stress relaxation of materials fabricated by additive manufacturing. Of importance are the findings on the relaxation properties described as a relationship between stress and time $\sigma = f(t)$ using rheological models, also called solid models [11, 12].

Many researchers dealing with stress relaxation of materials have tried to match the theoretical functions with the experimental functions; the results were satisfactory when single tests were considered. In the case of a series of tests, however, the problem is slightly more complex; it is essential either to estimate the uncertainty [1, 2, 13−16] or employ appropriate procedures of numerical analysis [17, 18].

This study is an attempt to solve the above problems by estimating the uncertainty of approximation of the relaxation parameters and by describing the relaxation curves by means of solid models and appropriate equations. The next sections provide details on fabrication of the specimens, performance of the relaxation tests and analysis of the results.

2. Experiment: materials and methods

The specimens were fabricated using digital materials, which were photocured resins sold under the commercial names VeroWhitePlus and TangoBlackPlus and a combination of the two, *i.e.* DM_9850_Shore50. The specimens were cylindrical in shape (D = 10 mm and H = 15 mm); they were produced with a Stratasys (Object) Connex350 3D printer using the PolyJet additive manufacturing technology (*http://www.stratasys.com/3d-printers/technologies/polyjet -technology*).

The experiments described in this paper were performed according to the procedure shown in Fig. 1.

The solid model of test pieces was generated in a 3D CAD program and saved as an *.stl* file. The settings determining the model accuracy selected in the STL Mesh Export Options dialogue box were as follows: resolution – adjusted, deviation – 0.016 mm tolerance, angle – 5^0 tolerance. Then, the Objet Studio program was used to arrange the models vertically on the build tray of the Connex350 printer. The specimens were printed in the Glossy mode to achieve smooth surfaces. Fig. 2 shows the models virtually distributed over the build tray in the Objet Studio program.

Once the printing was completed, the support material was removed. The specimens were tested for relaxation using an Inspekt mini universal testing machine [19]. The test parameters were set in the Labmaster program [20] integrated in the Inspekt mini machine. The test parameters were predetermined using block programming. The cylindrical specimens were compressed between two flat plates. They were placed vertically at the center of the lower plate. Then, the upper pressure plate mounted in the crosshead, held in the adapter, was lowered so that it touched the top flat surface of the specimens. The contact load did not exceed 10 N. All the readings, *i.e.* load, vertical travel, and time, were set to zero and the test started.
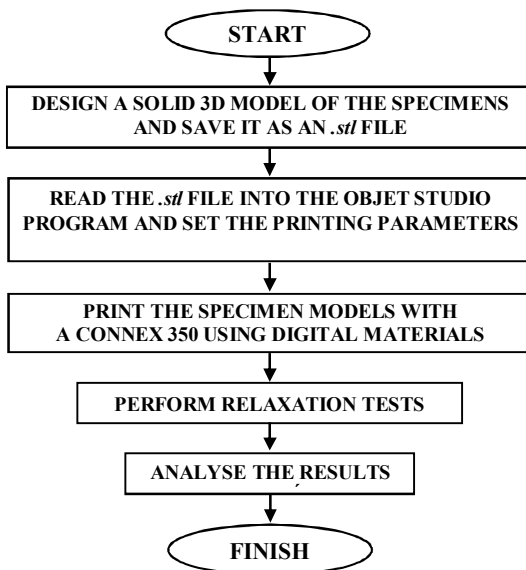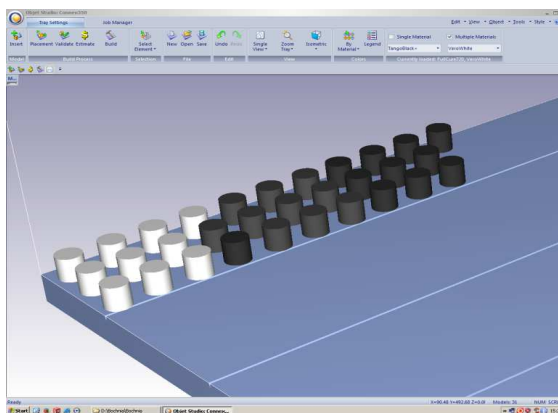
Fig. 1. Test procedure.

Fig. 2. The specimen models arranged on the build tray using the Objet Studio program.

In the first block, the displacement was set to 1 mm, with the displacement rate of the pressure plate being v = 10 m/min. The second block of the program involved stopping the pressure plate while maintaining a constant displacement of 1 mm for a predetermined time, *e.g.* 300 s. When the load force was reduced, the compressive stress decreased and stress relaxation occurred. The phenomena are presented graphically in the form of a curve. In the third block, the pressure plate returned to the initial (zero) position, and the load was removed. The whole relaxation test is illustrated graphically in Fig. 3.

The graph is divided into three regions. Region (1) represents a very rapid increase in load to achieve a 1 mm displacement. This abrupt change can be described mathematically with a unit step function. In real conditions, however, such a high rate of change is impossible to achieve. The load rate used in the tests was thus described using a quasi-unit step function (the almost vertical straight line 1 in Fig. 3). The next region represents the actual stress

relaxation process – line 2. Only this region of graph is considered in this analysis. The third region − the straight vertical line 3 − represents a rapid drop in load, and returning the upper plate to the initial (zero) position, which indicates the end of the test.

The stress relaxation tests were carried out for two elemental inks, TangoBlackPlus and VeroWhitePlus, and their combination, DM_9850_Shore50. Ten specimens were printed to represent each material in the relaxation tests.
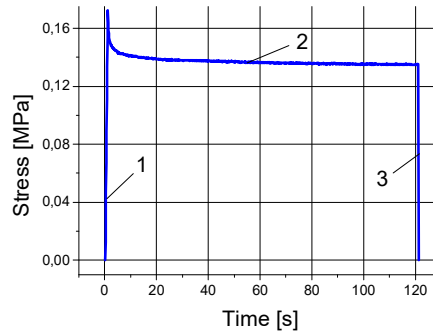

Fig. 3. A stress relaxation plot for DM_9850:
1 – load application (quasi-unit step function), 2 – stress relaxation, 3 – load removal.

It is very difficult to describe the relaxation process mathematically using a solid model as the description needs to have some physical significance. The relaxation curve is generally interpreted by means of the Maxwell model [21] or elements of the Maxwell model [11, 22, 23]. The classical relaxation curve is described using the generalized Maxwell model consisting of the Newtonian and Hookean models connected in series, which is expressed as:

$$\sigma(t) = \sigma_0 e^{\frac{-t}{t_1}},$$ (1)

where: σ_0 – the initial stress at $t = 0$; t_1 – the relaxation time.

The relaxation time, defined as a ratio of the properties of a Newtonian fluid and a Hookean solid, can be written as

$$t_1 = \frac{\mu_1}{E_1},$$ (2)

where: μ_1– the coefficient of viscosity; E_1 – the elastic modulus.

As the simple Maxwell model may be insufficient to approximate the experimental relaxation curve, more complex models need to be used. The generalized Maxwell model, also known as the Maxwell-Wiechert model, is shown in Fig. 4. The model consists of n simple Maxwell models assembled in parallel and Hooke's law, where $E_0, E_1, E_2 …E_n$ are the elastic moduli and $\mu_1, \mu_2, …\mu_n$ are the coefficients of viscosity of the simple models. The equation describing this model is written as:

$$\sigma(t) = \varepsilon_0 \left(\sum_{i=1}^{n} E_i e^{\frac{-t}{t_i}} + E_0 \right),$$ (3)

where: ε_0 – the predetermined displacement; n – the number of simple Maxwell models; i – the number of the subsequent model.

When $n = 1$, (3) will have the form:

www.czasopisma.pan.pl   PAN   www.journals.pan.pl
POLSKA AKADEMIA NAUK

Metrol. Meas. Syst., Vol. 23 (2016), No. 4, pp. 545–553.

$$\sigma(t) = \sigma_0 + \sigma_1 e^{\frac{-t}{t_1}}.$$ (4)

However, for $n = 2$, i.e. for two simple Maxwell models and Hooke's law assembled in parallel, (3) can be written as:

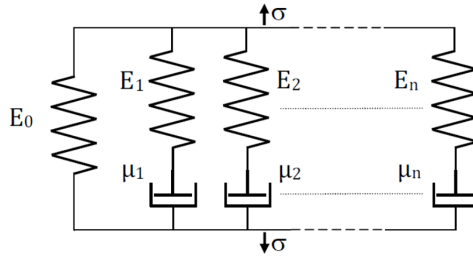$$\sigma(t) = \sigma_0 + \sigma_1 e^{\frac{-t}{t_1}} + \sigma_2 e^{\frac{-t}{t_2}}.$$ (5)

Fig. 4. The generalized Maxwell model (Maxwell-Wiechert model).

Figure 5 shows the experimental relaxation curve 2 from Fig. 3 compared with the curves obtained by approximation using (1, 2 and 3).
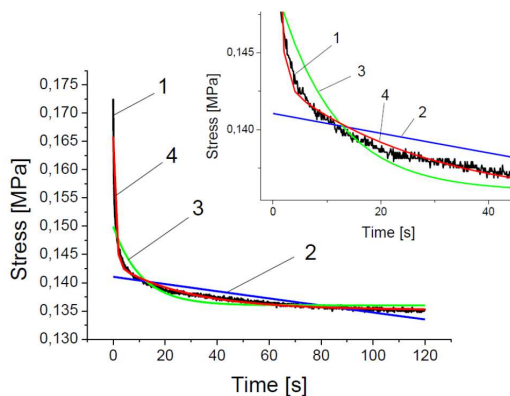

Fig. 5. The experimental curve compared with the approximation curves: 1 – the experimental curve for specimen 1 made of DM_9850, 2 – the approximation curve obtained using (1) for the simple Maxwell model, 3 – the approximation curve obtained using (4) for the Maxwell model and Hooke's law assembled in parallel, 4 – the approximation curve obtained using (5) for two Maxwell models and Hooke's law connected in parallel.

From the qualitative analysis presented in Fig. 5 it can be concluded that the best agreement of the approximation curve with the real (experimental) curve was obtained using (5). The usefulness of this equation and the quantitative goodness of fit of the curves were estimated by performing a series of relaxation tests; it was also essential to determine the standard deviation and the uncertainty of the approximation of the coefficients in (5).

3. Results and discussion

The cumulative relaxation curves obtained for the materials studied are shown in Fig. 6.
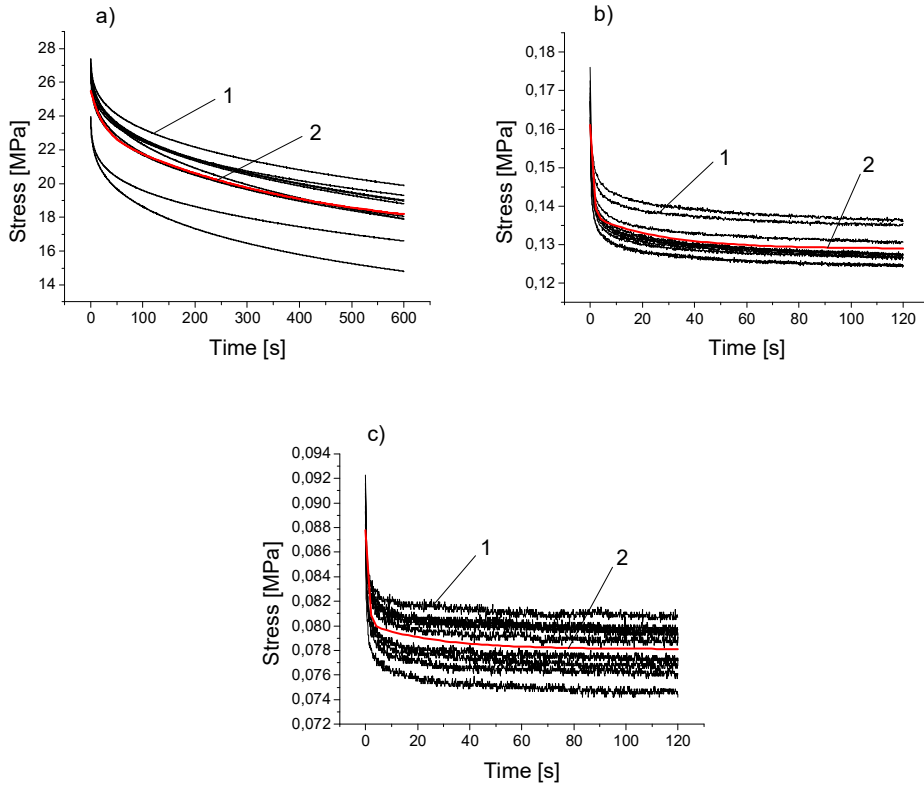
Fig. 6. The cumulative relaxation curves obtained for: a) VeroWhite; b) DM_9850_Shore50;
c) TangoBlackPlus. 1 – the experimental relaxation curves, 2 – the average relaxation curve approximated
using (5).

Each experimental relaxation curve was approximated by means of (5); that required determining the values of parameters σ_0, σ_1, σ_2, t_1 and t_2 and the values of chi-square and R-square tests. (5) was adjusted to obtain the best fit between the experimental data using the Origin program. The results are provided in Tables 1, 2 and 3.

Table 1. The parameters of the relaxation curves obtained for VeroWhite.

Test No.	σ_0 [MPa]	σ_1 [MPa]	σ_2 [MPa]	t_1 [s]	t_2 [s]	Chi^2	R^2
1	18.630	2.083	5.874	22.6	400.0	0.00163	0.99924
2	13.744	2.567	6.509	21.3	342.2	0.00261	0.99912
3	16.823	2.412	6.300	22.0	378.6	0.00208	0.99920
4	17.216	2.302	6.644	23.5	429.7	0.00191	0.99927
5	13.747	2.567	6.509	21.2	341.6	0.00261	0.99912
6	15.511	2.209	5.245	20.0	394.5	0.00219	0.99876
7	17.614	2.328	6.337	23.0	399.5	0.00194	0.99924
8	18.215	2.210	5.535	21.6	380.5	0.00186	0.99908
9	17.704	2.274	6.345	22.8	390.8	0.00190	0.99926
10	16.596	2.547	6.713	22.9	379.3	0.00234	0.99922
$\overline{X}$	**16.580**	**2.350**	**6.201**	**22.1**	**383.7**		

www.czasopisma.pan.pl   PAN   www.journals.pan.pl
POLSKA AKADEMIA NAUK

Metrol. Meas. Syst., Vol. 23 (2016), No. 4, pp. 545–553.

Table 2. The parameters of the relaxation curves obtained for DM_9850_Shore50.

Test No	σ_0 [MPa]	σ_1 [MPa]	σ_2 [MPa]	t_1 [s]	t_2 [s]	Chi2	R2
1	0.1352	0.0225	0.0082	0.88	27.82	1.87032E-7	0.97863
2	0.1247	0.0227	0.0084	0.82	26.50	1.80985E-7	0.97924
3	0.1248	0.0239	0.0082	0.77	24.09	1.87437E-7	0.97818
4	0.1276	0.0238	0.0092	0.85	27.93	1.93573E-7	0.98129
5	0.1277	0.0241	0.0085	0.85	25.86	2.05663E-7	0.97839
6	0.1269	0.0264	0.0082	0.84	23.28	1.89363E-7	0.98030
7	0.1271	0.0246	0.0085	0.85	26.66	2.25264E-7	0.97666
8	0.1310	0.0244	0.0087	0.81	24.86	2.14612E-7	0.97780
9	0.1365	0.0229	0.0094	0.94	30.18	2.05758E-7	0.98109
10	0.1278	0.0245	0.0102	0.84	26.30	2.08753E-7	0.98270
$\overline{X}$	**0.1289**	**0.0240**	**0.0087**	**0.84**	**26.35**		

Table 3. The parameters of the relaxation curves obtained for TangoBlackPlus.

Test No.	σ_0 [MPa]	σ_1 [MPa]	σ_2 [MPa]	t_1 [s]	t_2 [s]	Chi2	R2
1	0.0798	0.0070	0.0016	0.99	31.42	6.07481E-8	0.89845
2	0.0796	0.0075	0.0019	0.85	24.01	6.63337E-8	0.90596
3	0.0789	0.0080	0.0025	0.69	20.17	5.32286E-8	0.93512
4	0.0808	0.0068	0.0019	0.82	29.17	5.7908E-8	0.90540
5	0.0793	0.0077	0.0023	1.19	44.99	7.24707E-8	0.92552
6	0.0768	0.0083	0.0024	0.73	26.49	5.63208E-8	0.93483
7	0.0747	0.0078	0.0027	0.74	23.25	5.15685E-8	0.94535
8	0.0763	0.0078	0.0027	0.72	15.86	5.28378E-8	0.93842
9	0.0774	0.0078	0.0022	0.82	21.49	5.98535E-8	0.92328
10	0.0774	0.0078	0.0022	0.82	21.40	5.98448E-8	0.92329
$\overline{X}$	**0.0781**	**0.0077**	**0.0022**	**0.84**	**25.82**		

The standard deviation of parameters σ_0, σ_1, σ_2, t_1 and t_2 measured in each series was calculated using the following formula:

$$s = \sqrt{\frac{1}{(n-1)}\sum_{i=1}^{n}(x_i - \overline{x})^2}, \qquad (6)$$

where: n – the number of measurements (the number of specimens representing each material); x_i – the result in a series of measurements; $\overline{x}$ – the arithmetic mean obtained by approximation of each parameter.

The standard uncertainty calculated with a type A evaluation method is:

$$u_A = \sqrt{\frac{1}{n(n-1)}\sum_{i=1}^{n}(x_i - \overline{x})^2}. \qquad (7)$$

As the number of tested specimens was less than thirty (n = 10), the expanded uncertainty was calculated using the Student's t-distribution.

$$U_{CA} = k_p u_A, \qquad (8)$$

where: k_p – the coefficient of expansion, equal to 2 for the confidence level $p = 0.95$.

The measurement uncertainty and standard deviation values obtained for the tested materials are presented in Table 4.

Table 4. The approximation uncertainty and standard deviation.

Material	Approximation uncertainty U_{CA}					Standard deviation s				
	$U\sigma_0$ [MPa]	$U\sigma_1$ [MPa]	$U\sigma_2$ [MPa]	Ut_1 [s]	Ut_2 [s]	$s\sigma_0$ [MPa]	$s\sigma_1$ [MPa]	$s\sigma_2$ [MPa]	st_1 [s]	st_2 [s]
Vero White	1.094	0.106	0.31	0.6	16.8	1.728	0.169	0.490	1.08	26.55
DM_9850	0.0026	0.0008	0.0004	0.02	1.28	0.004	0.001	0.0007	0.04	2.01
Tango Black Plus	0.0012	0.0002	0.0002	0.1	5.12	0.0019	0.0004	0.0004	0.15	8.09

From the approximation uncertainty and standard deviation values given in Table 4 it is clear that the theoretical relaxation curves described with (5) are in a good agreement with the experimental relaxation curves. The low values of approximation uncertainty and standard deviation obtained for the selected parameters of relaxation curves result from the fact that the parameters, as shown in (2) and (3), are dependent on the material properties, *e.g.* the elastic moduli or the coefficients of viscosity represented by parameters σ_1, σ_2, t_1 and t_2, respectively, in (5). The curves in Figure 6 do not coincide, which is probably due to the technical difficulty to achieve a very high load rate (unit step function) during the relaxation tests. This also contributes to a higher uncertainty of measurement for parameter σ_0. The highest uncertainty of measurement for parameter σ_0 was obtained for VeroWhite, which is harder and stronger but less plastic than the other two materials. During the experiment, the stress occurred when the disc was in contact with a specimen. The stress was different for different specimens and it was definitely responsible for a higher uncertainty of measurement for parameter σ_0. The approximation uncertainty and the standard deviation were calculated to check the usefulness of the curve matching for the approximation curves compared with the experimental curves.

4. Conclusion

This paper has focused on the stress relaxation properties of cylindrical specimens fabricated with a 3D printer using the innovative PolyJet technology, which enables not only to create parts in different shapes and sizes but also to model the properties of the employed materials. The research project aimed to enrich knowledge of materials used in 3D printing.

The calculation results, *i.e.* the values of approximation uncertainty obtained for the parameters of relaxation function (5), were used to assess the coincidence of experimental curves; the analysis confirmed that the used solid model was suitable to define the properties of real material by comparing the experimental data with the theoretical results (curve matching). The description of experimental relaxation curves using the solid model and taking into account the uncertainty of approximation is of great significance because of the physical nature of the parameters. It also provides a better basis for modelling materials, especially digital materials, with predetermined relaxation properties or, more precisely, materials whose behavior is described by a rheological model.

References

[1] Adamczak, St., Bochnia, J., Kaczmarska, B. (2015). An analysis of tensile test results to assess the innovation risk for an additive manufacturing technology. *Metrol. Meas. Syst.*, 22(1), 127–138.

[2] Adamczak, S., Bochnia, J., Kaczmarska, B. (2014). *Estimating the uncertainty of tensile strength measurement for a photocured material produced by additive manufacturing*, 21(3), 553–560.

www.czasopisma.pan.pl   PAN   www.journals.pan.pl
POLSKA AKADEMIA NAUK

Metrol. Meas. Syst., Vol. 23 (2016), No. 4, pp. 545–553.

[3] Chockalingam, K., Jawahar, N., Chandrasekhar, U. (2006). Influence of layer thickness on mechanical properties in stereolithography. *Rapid Prototyping Journal*, 12(2), 106–113.

[4] Ahn, S.-H., Montero, M., Odell, D., Roundy, S., Wright, P.K. (2002). Anisotropic Material Properties of Fused Deposition Modeling ABS. *Rapid Prototyping*, 8(4), 248–257.

[5] Raut, S., Jatti, V.S., Khedkar, N.K., Singh, T.P. (2014). Investigation of the Effect of Built Orientation on Mechanical Properties and Total Cost of FDM Parts. *Procedia Materials Science*, *Elsevier B.V*., 6 No. Icmpc, 1625–1630.

[6] Lee, C.S., Kim, S.G., Kim, H.J., Ahn, S.H. (2007). Measurement of anisotropic compressive strength of rapid prototyping parts. *Journal of Materials Processing Technology*, 187–188, 627–630.

[7] Fernandes, V.A., De Focatiis, D.S.A. (2014). The role of deformation history on stress relaxation and stress memory of filled rubber. *Polymer Testing*, 40, 124–132.

[8] Chivers, R.A., Bonner, M.J., Hine, P.J., Ward, I.M. (2014). Shape memory and stress relaxation behaviour of oriented mono-dispersed polystyrene. *Polymer*, 55, 1055–1060.

[9] Luheng Wang, L., Han, Y. (2013). Compressive relaxation of the stress and resistance for carbon nanotube filled silicone rubber composite. *Composites Part A*, 47, 63–71.

[10] Stan, F., Fetecau, C. (2013). Study of stress relaxation in polytetrafluoroethylene composites by cylindrical macroindentation. Composites Part B, 47, 298–307.

[11] Hernández-Jiménez, A., Hernández-Santiago, J., Macias-Garcìa, A., Sánchez-González, J. (2002). Relaxation modulus in PMMA and PTFE fitting by fractional Maxwell model. *Polymer Testing*, 21, 325–331.

[12] Colucci, D.M., O'Connell, P.A., McKenna, G.B. (1997). Stress relaxation experiments in polycarbonate: a comparison of volume changes for two commercial grades. *Polym. Eng. Sci*., 37(9), 1469–1474.

[13] Bąkowski, A., Radziszewski, L. (2015). Determining selected diesel engine combustion descriptors based on the analysis of the coefficient of variation of in-chamber pressure. *Bulletin of the Polish Academy of Sciences technical sciences*, 62(2), 457–464.

[14] Kisała, P. (2012). Metrological conditions of strain measurement optoelectronic method by the use of fibre bragg gratings. *Metrol. Meas. Syst.*, 19(3), 471–480.

[15] Sładek, J., Gąska, A., Olszewska, M., Kupiec, R., Krawczyk, M. (2013). Virtual Coordinate Measuring Machine butli Rusing Laser Tracer system and spherical standard. *Metrol. Meas. Syst.*, 20(1), 77–86.

[16] Krawczyk, M., Gąska, A., Sładek J. (2015). Determination of the uncertainty of the measurements performer by coordinate measuring machines. *Technisches Messen*, 82(6), 329–338.

[17] Błasiak, S., Kundera, Cz., Bochnia, J. (2011). A Numerical Analysis of the Temperature Distributions in Face Sealing Rings. *Procedia Engineering*, 39, 366–378.

[18] Stępien, K., Janecki, D., Adamczak, S. (2011). Investigating the influence of selected factors on results of V-block cylindricity measurements. *Measurement*, 44(4), 767–777.

[19] Inspekt Mini (2011). Universal testing machine Inspekt mini 3kN, Hegewald & Peschke MPT GmbH.

[20] LabMaster software (2011). Version 2.5.3.21.

[21] Del Nobile, M.A., Chillo, S., Mentana, A., Baiano, A. (2007). Use of the generalized Maxwell model for describing the stress relaxation behavior of solid-like foods. *Journal of Food Engineering*, 78, 978–983.

[22] Kai-Xin, H., Ke-Qin, Z. (2011). A note on fractional Maxwell model for PMMA and PTFE. *Polymer Testing*, 30, 797–799.

[23] Tingting, H., Hongshan, C. (2012). Isothermal physical aging of PEEK and PPS investigated by fractional Maxwell model. *Polymer*, 53, 2509–2518.